AUTHOR(S): SHARMA, L., LONE, N.A., KNOTT, R.M., HASSAN, A. and ABDULLAH, T.

TITLE: Trigonelline prevents high cholesterol and high fat diet induced hepatic lipid accumulation and lipo-toxicity in C57BL/6J mice, via restoration of hepatic autophagy.

YEAR: 2018

Publisher citation: SHARMA, L., LONE, N.A., KNOTT, R.M., HASSAN, A. and ABDULLAH, T. 2018. Trigonelline prevents high cholesterol and high fat diet induced hepatic lipid accumulation and lipo-toxicity in C57BL/6J mice, via restoration of hepatic autophagy. Food and chemical toxicology [online], 121, pages 283-296. Available from: https://doi.org/10.1016/j.fct.2018.09.011

OpenAIR citation: SHARMA, L., LONE, N.A., KNOTT, R.M., HASSAN, A. and ABDULLAH, T. 2018. Trigonelline prevents high cholesterol and high fat diet induced hepatic lipid accumulation and lipo-toxicity in C57BL/6J mice, via restoration of hepatic autophagy. Food and chemical toxicology, 121, pages 283-296. Held on OpenAIR [online]. Available from: https://openair.rgu.ac.uk

Accepted Manuscript

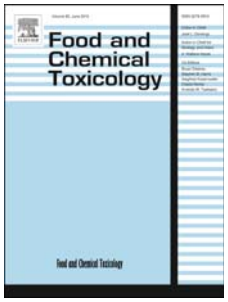

Trigonelline prevents high cholesterol and high fat diet induced hepatic lipid accumulation and lipo-toxicity in C57BL/6J mice, via restoration of hepatic autophagy

Love Sharma, Nazir A. Lone, Rachel M. Knott, Adil Hassan, Tasduq Abdullah

PII: S0278-6915(18)30655-0

DOI: 10.1016/j.fct.2018.09.011

Reference: FCT 10037

To appear in: *Food and Chemical Toxicology*

Received Date: 24 May 2018

Revised Date: 6 September 2018

Accepted Date: 7 September 2018

Please cite this article as: Sharma, L., Lone, N A., Knott, R M., Hassan, A., Abdullah, T., Trigonelline prevents high cholesterol and high fat diet induced hepatic lipid accumulation and lipo-toxicity in C57BL/6J mice, via restoration of hepatic autophagy, Food and Chemical Toxicology (2018), doi: 10.1016/j.fct.2018.09.011.

Trigonelline prevents high cholesterol and high fat diet induced hepatic lipid accumulation and lipo-toxicity in C57BL/6J mice, via restoration of hepatic autophagy.

Love Sharma[1, 2], Nazir A Lone[1,2], Rachel M Knott[3], Adil Hassan [4], Tasduq Abdullah[1,2].

[1]Academy of Scientific and Innovative Research (AcSIR), Jammu Campus, CSIR-Indian Institute of Integrative Medicine, Canal Road, Jammu Tawi, Jammu and Kashmir, India.

[2]PK-PD and Toxicology Division, CSIR-Indian Institute of Integrative Medicine, Canal Road, Jammu Tawi, Jammu and Kashmir, India.

[3]School of Pharmacy and Life Sciences, Robert Gordon University, Aberdeen, Scotland, UK.

[4]Department of Pathology, Government Medical College, Srinagar, Jammu and Kashmir, India.

Correspondence: Dr. Tasduq Abdullah

Address: PK-PD Toxivcology Division

Indian Institute of Integrative Medicine, CSIR-IIIM

Canal Road, Jammu, Jammu and Kashmir

Pin/Zip : 180001, India

E-mail: stabdullah@iiim.ac.in

Contact: +91-9419148712

Abstract

Non-alcoholic fatty liver disease (NAFLD) is often linked with impaired hepatic autophagy. Here, we studied the alterations in hepatocellular autophagy by high cholesterol and high-fat diet (HC-HF) diet in C57BL/6J mice, and by palmitic acid (PA), in AML-12 and HepG2 cells. Further, we analysed role of Trigonelline (TG), a plant alkaloid, in preventing NAFLD, by modulating autophagy. For this, C57BL/6J mice were fed with Standard Chow (SC) or HC-HF diet, with and without TG for 16 weeks. *In-vitro*; AML-12 cells and HepG2 cells, were exposed to PA with and without TG, for 24 hours. Cellular events related to autophagy, lipogenesis, and lipo-toxicity were studied. The HC-HF diet fed mice showed hepatic autophagy blockade, increased triglycerides and steatosis. PA exposure to AML-12 cells and HepG2 cells induced impaired autophagy, ER stress, resulting in lipotoxicity. TG treatment in HC-HF fed mice, restored hepatic autophagy, and prevented steatosis. TG treated AML-12, and HepG2 cells exposed to PA showed autophagy restoration, and reduced lipotoxicity, however, these effects were diminished in Atg7-/- HepG2 cells, and in the presence of chloroquine. This study shows that HC-HF diet-induced impaired autophagy, and steatosis is prevented by TG, which attributes to its novel mechanism in treating NAFLD.

Keywords: Trigonelline, Autophagy, NAFLD.

1. **Introduction**

Non-alcoholic fatty liver disease (NAFLD), and its associated co-morbidities are one of the defining ailments of the current time (Trovato et al., 2016). NAFLD ranges from steatosis to more severe form, i.e., non-alcoholic steatohepatitis (NASH) (Wree et al., 2013). NAFLD reported to have a prevalence of 20-30 % and 15-20% in the West, and in Asia respectively (Bellentani et al., 2010). Many factors contribute to the development of NAFLD, including perturbances in insulin signalling and cellular pathways viz. m-TOR, autophagy, AMPK, etc. (Berlanga et al., 2014). Autophagy is a lysosomal degradation pathway of the cell and plays a critical role in many physiological and pathological conditions, (Ouyang et al., 2012). It is activated during the starving state, of the cell, and acts to switch off nutrient overload via mTOR in-activation (Alers et al., 2012). Further, m-TOR and AMPK pathways share a link with insulin signalling, and the interplay between mTOR, AMPK, and insulin signalling plays a critical role in the development of NAFLD (Quan et al., 2013). NAFLD is also associated with several co-morbidities, like type 2 diabetes mellitus (T2DM), with both conditions involving insulin resistance (IR), glucose and lipid metabolism in adipocytes and hepatocytes (Gaggini et al., 2013). Peripheral insulin resistance (PIR) leads to enhanced lipolysis and excess entry of fatty acids to the liver, whereas hepatic insulin resistance (HIR) itself accelerates *de novo*-lipogenesis in the liver, both leading to NAFLD. Chronic HIR leads to activation of mTOR in hepatocytes, thereby increasing *de novo* lipogenesis and shuts down the hepatic autophagy (Kim et al., 2011; Um et al., 2006). Another, important aspect of fatty liver, is lipid droplets (LDs), which were conventionally considered for their role, only in energy storage but, recent studies have suggested that LDs, are dynamic organelles, which may have a variety of functions, and play a critical role in etiopathogenesis of various diseases including NAFLD (Greenberg et al., 2011). A study has demonstrated that LDs can be a substrate for autophagy, and act as mobile organelles for the lipids, for its degradation by

the process known as lipophagy. This study showed that lipophagy play a central role in hepatic lipid metabolism, and defect in the process of lipophagy leads to accumulation of LDs, which contributes significantly in the development of fatty liver (Singh et al., 2009). Inhibition of autophagy in hepatocytes showed increased LDs accumulation (Nissar et al., 2017) following the use of pharmacological-autophagy inhibitors viz. chloroquine (CQ), 3-methyl adenine (3-MA), and Bafilomycin led to increasing in LDs (Nissar et al., 2017). These findings suggest that targeting hepatic lipophagy could treat fatty liver. Many such natural hepatic autophagy stimulators have shown beneficial effects on the resolution of liver fat, which includes resveratrol (Zhang et al., 2015), caffeine (Sinha et al., 2014), 4-PBA (Nissar et al., 2017), etc. One of the natural plant alkaloids is Trigonelline (TG), which is yet to be tested as a hepatic lipophagy stimulator, for preventing fatty liver. It is present in the variety of edible natural products which are routinely consumed by humans. It is reported to have anti-carcinogenic, anti- hypercholesterolemic, and anti-diabetic activities (Anthoni et al., 1991). In humans, TG is a metabolite of niacin, which is a part of various vitamins based nutraceutical products, and is used for its anti-dyslipidemic activity (Ghule et al., 2012). It is also a potent anti-oxidant, as it has shown prevention from quite a few disorders, arising out of oxidative stress and generation of reactive oxygen species (ROS). TG reduced the diabetic hypertensive nephropathy in kidney and also showed protection to the cardiocytes from hydrogen peroxide (Ghule et al., 2012),(Tharaheswari et al., 2014). Many *in-vivo* studies have evaluated its effectiveness for diabetes, and the regulation of hyperglycemia and its anti-oxidant properties are also well known (Zhou et al., 2012; Zhou et al., 2013) but data to prove its effectiveness in preventing fatty liver is lacking. Previously, we have shown that agents which induce mTOR inhibition and autophagy induction prevent LDs accumulation in PA exposed hepatocytes and high-fat diet fed C57BL/6J mice (Love et al., 2017; Nissar et al., 2017). In this, study we have evaluated TG in preventing the development of NAFLD by

employing 16 weeks high cholesterol, high-fat and fructose diet [HC-HF} model in C57BL/6J mice. Further, the effects of TG were assessed on palmitate stimulated mouse hepatocytes (AML-12) and human hepatoma cells (HepG2). The modulation of the molecular pathological events by TG, related to NAFLD was evaluated concerning autophagy machinery, endoplasmic reticulum (ER) stress, and *de novo* lipogenesis in hepatic cells.

2. Materials and Methods

2.1 Cell Culture and treatments:

Mouse hepatocytes AML-12 cells and human hepatoma cells (HepG2) were purchased from ATCC USA. Cells were maintained and propagated in DMEM media (Sigma-Aldrich, USA) supplements with 10% FBS (Gibco, USA). The AML-12, cells were additionally supplemented with 1% Insulin-selenium-transferrin (Sigma-Aldrich, USA) as recommended. Cells were used at a density of 5 x 10^4 cells/24 well plate, 7 x 10^5 cells/6 well plate or 1.2 x 10^6 cells/60mm dish (Nunc, USA) unless otherwise specified. All studies were conducted using 70-80% confluent cells, which were treated with specified concentrations of sodium palmitate (PA) (Sigma Aldrich, MO, USA) for 24 hours. For treatment, AML-12 cells and HepG2 were grown in 60 mm culture dishes (Nunc, USA). Cells were pre-treated with TG (25 μM and 50 μM) (4 hours before PA exposure) and co-treated with TG (25 μM and 50 μM) along with PA (Sigma Aldrich, MO, USA) as indicated. CQ at 100 μM for RFP-GFP-LC3B and 50 μM for other experiments, 3-methyl adenine (3-MA) at 2mM and Everolimus (EV) at 100nM (Sigma Aldrich, MO, USA) were exposed to cells as indicated, for 1 hour before to PA addition, and then in combination with the PA. The optimisation of *in-vitro* working concentration of TG is described in the results section.

2.2 PA-Bovine Serum Albumin [BSA] mixture preparation:

PA and BSA [Sigma Aldrich, MO, USA] were combined to make a 1mM stock solution of PA which was subsequently used for all experiments as previously (Nissar et al., 2015).

2.3 Cell viability assay:

The viability of AML-12 cells was determined by MTT assay 3-(4,5-Dimethylthiazol-2-yl)-2,5-diphenyltetrazolium bromide (Sigma Aldrich, MO, USA) as previously described (Nissar et al., 2015). After 24 hours of respective treatments, cells were incubated with MTT solution (0.25mg/ml in PBS) for 3 hours at 37° C. Formazan crystals formed by cells were dissolved in DMSO, and optical density was recorded at 570nm using a plate reader (Multiskan Spectrum; Thermo Electron Corporation, USA).

2.4 Measurement of mitochondrial membrane potential ($\Delta\Psi m$).

AML-12 cells were stained with JC-9 (5 μg mL^{-1}) and imaging of cells was done according to an established protocol to determine any changes (Farrukh et al., 2014). Briefly, AML-12 cells were cultured and at about 50–60% confluency, cells were treated with either PA (250μM) alone or with TG (25μM and 50μM). After 24 hours, DMEM containing 5 μg mL−1 JC-9 (Sigma Aldrich, St. Louis, MO) was pre-warmed to 37 °C and then added to the cells and incubated for 30 minutes at 37 °C in a CO_2 incubator. The medium was removed, and the cells were washed three times with Dulbecco Phosphate Buffer Saline (DPBS) (pre-warmed at 37 °C). Imaging was done using a laser scanning confocal microscope (Olympus FluoView FV-1000).

2.5 Mono-dansylcadaverine (MDC)

Mono-dansylcadaverine dye (Cat No. – 30432), is an auto-florescent dye, which is used to detect autophagy in cells. It helps in detecting autophagosomes, by its ability to concentrate in the autophagic vacuoles, by various mechanisms, involving interactions with the cellular lipids, and ion-trapping. The autophagosomes accumulation represent autophagy blockade,

due to less degradation of cargo in the form of autolysosomes. Higher the intensity of MDC stain, has been shown to be directly proportional to the accumulation of autophagosomes (Biederbick et al., 1995). For MDC staining, cells were incubated with 50µM MDC solution prepared in PBS at 37°C for 1 hour. Post-incubation cells were washed three times in PBS and immediately analysed by fluorescence microscope using 40X lens.

2.6 Lysotracker green-Nile Red co-staining.

Lysotracker is an acidotrophic dye, which is used for sub-cellular localization of lysosomes, and auto-lysosomes in the live cells. It can accumulate in low ph compartments of the cells. This staining is used for detecting autophagy process, especially its degradation step. The higher intensity of lysotracker dye, indicates the presence of more lysosomes, indicating stimulated autophagy flux, (Chazotte, 2011) (Rah et al., 2015). For this, cells were stained with 300nM Lysotracker green dye (Invitrogen, L7526) solution in DMEM media, for 45 minutes at 37°C. The cells were washed with PBS thrice and co-stained with Nile Red solution (5ng/µl) for 5 minutes, washed again thrice with PBS and analysed immediately by fluorescence microscope 40X lens. The co-staining of Lysotracker and Nile red dye provided the important link between autophagy machinery of cells and LDs accumulation. The imaging was done by Evos (Life Technology) microscope.

2.7 Small interfering RNA-mediated knockdown of Atg7.

Validated Atg7 small interfering RNA (siRNA) (Santa Cruz Biotechnology, USA).SiRNA and Lipofectamine (Invitrogen) were diluted into Opti-MEM I reduced serum medium (Invitrogen) as per manufacturer's instructions. HepG2 cells were incubated for 16 hours with a transfection mixture at a final siRNA concentration of 50pmol and then supplemented with fresh medium and further, TG and palmitic acid treatments as described.

2.8 p62 immunostaining-Nile red co-staining

This imaging was performed to understand the association of autophagy flux and accumulation of LDs in the cell. The co-staining of cell with Nile-red, immunostained with p62, provides the link between autophagy blockade or autophagy induction with the accumulation of LDs. For this AML-12 cells were seeded in chamber slides (Nunc, Thermo) and after attaining the desired confluency, the indicated treatments were given. The chloroquine (CQ) was used as a positive control of being an autophagy inhibitor. The immunostaining protocol for p62 was followed as described previously (Nissar et al., 2017). The Alexa Flour 488, conjugated secondary anti-rabbit (Invitrogen, Thermo-Fisher) antibody was used, followed by co-staining with Nile-red (as described earlier) and DAPI dye. Imaging was done by fluorescence microscopy at 40X lens, by Evos (Thermo-Scientific, USA).

2.9 Beclin1 immunostaining

For this, cells were seeded in chamber slides (Nunc, Thermo) and after attaining the desired confluency, the indicated treatments were given. The immunostaining protocol for beclin-1 was followed as described previously (Nissar et al., 2017). The Alexa Fluor 594 conjugated anti-rabbit secondary antibody (Invitrogen) was used, followed by co-staining with DAPI dye. AML-12 cells were imaged by fluorescence microscopy at 40X lens, by Evos (Thermo-Scientific, USA).

2.10 RFP-GFP-LC3B puncta assay

This assay was performed to analyse the autophagic flux. This assay is used to analyse the cellular autophagy via LC3B protein localization. This assay was performed by using Premo™ Autophagy Tandem Sensor RFP-GFP-LC3B Kit (Cat No. P36239, Invitrogen, Thermo-Fisher). This kit is a simplified version of mGFP-eGFP-LC3 constructs. The chimera

of kit contains TagRFP and Emerald GFP proteins, complexed with LC3B. The GFP-RFP sensor works on between acidic autolysosomes and neutral autophagosomes. The difference in the pH, helps in monitoring the conversion of autophagosomes to autolysosomes, as GFP and RFP proteins here are pH sensitive (Huang et al., 2015; Perez-Neut et al., 2016). For this, AML-12 cells, upon achieving the desired confluency, were infected with Bacman 2.0 RFP-GFP-LC3B reagent (12µl for 40, 000 cells, as per manufacturer instructions) for 16 hours, followed by the treatments. The CQ was used at 100µM (as per manufacturer instructions) as a positive control. The cells were co-stained with DAPI dye. The imaging was performed by using fluorescence microscopy, EVOS (Thermo-Fisher) by employing GFP, RFP and DAPI filters, at 40X.

2.11 Determination of reactive oxygen species (ROS)

AML-12 cells were seeded in 60mm culture dishes, and after attaining the desired confluency, cells were treated as indicated, for 24 hours. Cells were washed, incubated with 5µM H_2DCF-DA for 30 minutes at 37°C. Imaging was done by fluorescence microscopy at 20X lens, Evos (Thermo-Scientific, USA) using green filters. Image quantification was carried out by using Image J software, as previously (Nissar et al., 2015).

2.12 Animals and Treatments

C57BL/6J, Male mice, 4 to 6 weeks old, genetically un-altered were procured from CSIR-Indian Institute of Integrative Medicine (IIIM) animal breeding facility and maintained within the facility under 12 hours light/dark cycle. The mice were acclimatized for one week, before the start of the study. The study and the related procedures were approved by the institutional animal ethical clearance committee (IAEC). The HC-HF diet used in this study have been described in detail previously (Nissar et al., 2015). The mice were divided into four groups (n=6). Group 1 [Standard Chow (SC) Diet], Group 2 [High Cholesterol and High Fat diet

[HC-HF] diet], Group 3 [HC-HF + TG (50mg/kg)], Group 4 [SC+TG (50mg/kg)]. The TG was administered a week thrice by oral gavaging by preparing freshly in the Type-1 filtered water on every dosing schedule. The animals within Group 1 and 2 were administered water without TG. Diet and water were given ad-libitum. The dose of TG, i.e., 50mg/kg was selected based on the previous studies (Folwarczna, 2016; Zhou et al., 2013). The TG has been used in a range of 50mg/kg to 100mg/kg in mice and rats (Ghule et al., 2012). The toxicological data available for TG, also reported that sub-chronic exposure of TG at 50mg/kg orally for 21 days to albino Sabara rats did not reveal any signs of toxicity (Zeiger and Tice, 1997). Hence, we selected the physiological dose of 50mg/kg of TG. As the study was for 16 weeks, the dosing was done three times a week, to ensure minimal adverse drug affects (if any). The day before termination, mice were fasted for 12 hours, and sacrificed by Co_2 inhalation. The blood and liver samples were collected. The harvested livers were washed, perfused, weighed and the largest lobe of the livers was sliced, either for snap freezing in liquid nitrogen, for molecular and protein analysis, and/or stored in 10% formalin, for further paraffin sectioning and histological analysis. Blood samples were centrifuged, and serum was collected, either for immediate colorimetric analysis of serum biochemistry (Glucose, Triglycerides and Cholesterol) or stored in -80^{o} C, for later analysis of serum insulin levels by ELISA as described below.

2.13 Western Blotting

Approximately, 30mg of liver tissue was taken from each of four mice, which were selected randomly from each group. Tissue was micronized by hand homogenizer (D-1, MICCRA, Germany) in a modified lysis buffer ; the protein was extracted as described previously (Love et al., 2017). For, cell protein lysates AML-12 cells or HepG2 cells, were trypsinized, collected and re-suspended in radio-immunoprecipitated assay (RIPA) buffer (Sigma Aldrich,

MO, USA) for protein extraction, and western blot protocol was followed as described previously (Love et al., 2017).Quantification of blots was carried out by densitometry using Image Lab™ software, version 3.0, Bio-Rad (Hercules, CA, USA). The following primary antibodies were employed, to study a) ER stress pathways (anti-GRP78, anti-CHOP, anti-p-elf2alpha, anti-total elf2alpha), b) Apoptotic studies (anti-PARP, anti-BCL-2, anti-Bax), c) Lipogenesis and insulin signalling (anti-p-mTOR, anti-mTOR, anti-p-Akt, anti-Akt, anti-Srebp1, anti-PPAR-gamma, anti-perilipin, anti-CD36), c) Autophagy pathway (anti-BECN and anti-SQSTQM1/p62 (Santa-Cruz Biotechnology, USA) anti-p-AMPK, anti-AMPK, anti-Atg5, anti-Atg7, (Cell Science and Technology, USA) and anti-LC3-II), d) Internal Control (anti-Beta-Actin (Sigma-Aldrich, MO, USA).

2.14 Nile red staining, Haematoxylin & Eosin (H&E) staining

Nile red staining was performed to access the lipid accumulation in livers of C5BL/6J mice and in AML-12 cells when treated with various indicated treatments, as per the protocol described in (Nissar et al., 2015). The H&E staining was performed as per the laboratory protocol described previously (Love et al., 2017). The slides were examined by the professional pathologist who was blinded to the study.

2.15 Serum Biochemistry

The serum glucose, serum triglyceride (Trig), serum cholesterol was analysed by colorimetric assay by using designated colorimetric kits (ERBA, Transasia, India), as per manufacturer's protocol. Serum insulin was performed by ELISA assay by using mouse insulin ELISA kit (Millipore), as per manufacturer protocol.

2.16 Triglyceride (Trig) estimation in the liver and AML-12 cells.

Trig extraction from the livers of C57BL/6J mice and from AML-12 cells was done by using LPL buffer, as described in (Love et al., 2017; RodrÃ-guez-Sureda and Peinado-Onsurbe, 2005) and analysed by using colorimetric method.

2.17 Statistical Analysis

Statistical analysis was performed by using INSTAT statistical software. Data are represented as Mean ± S.E. from three independent experiments. Statistical comparisons between two groups were performed by student *'t'* test and among groups by One-way ANOVA. $p \leq 0.05$ was considered as statistically significant.

3. Results

3.1 Effect of TG on cellular viability

The cellular viability of AML-12 cells was in the range of 99.44% to 99.62 % at 25-50µM concentrations after 24 hours of TG exposure and at higher doses, there was a decrease in cellular viability, although insignificant, Figure 1a. Further, the *in-vitro* doses for TG have been used in a range of 75µM and 100µM, for studying adipocyte differentiation and lipid accumulation in 3T3-L1 cells (Ilavenil et al., 2014). TG didn't affect the cell viability of H9C2 cells, in range of 25-100µM concentration after 24 hours (Ilavenil et al., 2015). We analysed the anti-lipotoxic and anti-steatotic potential of TG at 25µM and 50µM on PA exposed AML-12 cells, which proved to be effective (discussed in next heading) Figure 1b, 1c, and 1d. Hence, these two doses of TG were carried forward for the further experiments.

3.2 TG prevented PA-induced lipo-toxicity and lipid accumulation in AML-12 cells.

AML-12 cells were exposed to PA-250µM (Love et al., 2017) for 24 hours, and it induced cytotoxicity significantly by 33.28% ($p<0.01$, Pa Vs. Control), Figure 1b. In TG treated PA

exposed cells, the cell viability was increased at TG (25μM and 50μM) by 12.38 % (p<0.05, PA Vs. PA + TG 25μM/50μM), Figure 1b. Further, ΔΨm was hyperpolarized due to PA exposure, as shown by enhanced red fluorescence, (p<0.001, Control Vs. PA) and low green fluorescence, whereas in TG treated cells, there was no change in ΔΨm (p< 0.001, PA Vs. PA + TG 25 μM/50 μM), Figure 1c. We analysed lipid accumulation via Nile red staining. The higher fluorescence intensity suggested excessive LDs accumulation in PA exposed cells (*** represents p<0.0001, PA Vs. Control). Treatment with TG (25μM and 50μM) prevented PA-induced lipid accumulation, evident from 1.5 times decreased fluorescence intensity, compared to PA exposed cells ($^{###}$ represents p< 0.0001, PA Vs. PA + TG 25 μM/50 μM), Figure 1d, 1e.

3.3. PA-induced ER stress and apoptosis in AML-12 cells, which was reduced by TG treatment.

After 12 hours of PA exposure to AML-12 cells, the protein expressions of ER stress markers viz. GRP-78, p-elf-2α, CHOP and ATF-4, were up-regulated as compared to unexposed control cells (*** represents p< 0.0001, PA Vs. Control for GRP-78 and elf-2α) Figure 2a, 2d. ER stress induction by PA in AML-12 cells was associated with the generation of reactive oxygen species (ROS), which was confirmed by enhanced green fluorescence via the H2DCF-DA imaging in PA exposed cells, Figure 2b. TG treatment prevented PA-induced ER and oxidative stress in AML-12 cells. The GRP-78 and elf-2α were down-regulated significantly ($^{##}$ represents p< 0.001, PA Vs. PA + TG 25 μM/50 μM for GRP-78 and $^{#}$ represents p< 0.05, PA Vs. PA + TG 25 μM/50 μM for elf-2α), in TG treated cells exposed to PA, Figure 2a, 2d. TG treatment also prevented the ROS generation in AML-12 cells exposed to PA, Figure 2b. Further, PA-induced lipo-toxicity was verified by low levels of the apoptotic markers, i.e., bcl-2/bax as compared to control cells, along with significant

cleavage of PARP, (*** represents $p< 0.0001$ PA Vs. Control), Figure 2c, 2d. However, in TG treated cells, the bcl-2/bax ratio was significantly up-regulated as compared to PA exposed cells ($^{\#\#}$ represents $p< 0.001$, PA Vs. PA + TG 25 µM/50 µM), and cleavage of PARP was also significantly lesser than PA exposed cells ($^{\#}$ represents $p< 0.05$, PA Vs. PA + TG 25 µM, $^{\#\#}$ represents $p<0.001$, PA Vs. PA + TG 50µM).

3.4 TG prevented up-regulation of de-novolipogenesis in AML-12 cells exposed to PA.

De novo lipogenesis contributes significantly to promoting lipid storage in the liver, and it is activated by intake of high caloric diets (Diraison et al., 2003). The mTOR, is the main regulator of lipogenesis (Laplante and Sabatini, 2009) was activated by PA in AML-12 cells, as the ratio of protein expression of p-mTOR/mTOR was 1.7-fold higher in PA exposed cells as compared to control (** represents $p< 0.001$ PA Vs. control cells), Figure 3a, 3d. TG treatment prevented the m-TOR up-regulation in AML-12 cells ($^{\#}$ represents $p< 0.05$ PA Vs. PA + TG 25 µM/50µM), Figure 3a, 3d. The mTOR activation further activates nuclear receptors proteins viz. PPAR-γ, SREBP1 which execute the lipogenesis (Laplante and Sabatini, 2009). The protein expressions of both PPAR-γ and SREBP1 were increased by the PA exposure (*** represents p< 0.0001 PA Vs. Control for SREBP1 and ** represents p< 0.001 PA Vs. Control for PPAR-γ), whereas in TG treated cells, there were significant down-regulations of PPAR-γ and SREBP1 ($^{\#\#\#}$ represents p< 0.0001 PA Vs. PA+TG 25µM/50 µM, for SREBP1 and $^{\#\#}$ represents p< 0.001 PA Vs. PA+TG 25 µM/50 µM for PPAR- γ), Figure 3b, 3d. The Perilipin helps in adhesion of LDs, (Heid et al., 2014) while CD36 contributes to fatty acids translocation into the hepatocytes (Miquilena-Colina et al., 2011). Expressions of both Perilipin and CD36 expression were significantly increased in PA exposed cells, (*** represents p< 0.0001 PA Vs. Control, for Perilipin & CD36), Figure 3b. As expected,

expression of Perilipin and CD36 was reduced in TG treated PA exposed cells, and it was comparable with the untreated control cells, Figure 3b, 3d.

3.5 PA-induced lipid accumulation was associated with hepatic autophagic block, which was prevented by TG treatment by restoring autophagy.

MDC staining of PA exposed AML-12 cells showed autophagosomes accumulation, Figure 3h. Exposure of PA in AML-12 cells, led to reduced phosphorylation of AMPK and subsequently low expression of AMPK, Figure 3c, 3e (** represents $p< 0.001$ PA Vs. Control), followed by significant p62 accumulation (*** represents $p< 0.0001$ PA Vs. Control) significantly lower expression of Atg7, Figure 3c, 3e. Beclin-1 plays a crucial role in executing autophagy, it was also decreased significantly by PA exposure in AML-12 cells, Figure 3c, 3e, 3f. PA-induced autophagy blockade was also confirmed by the enhanced GFP-LC3B protein expression and negligible RFP-LC3B expression, studied by RFP-GFP-LC3B vector puncta assay. The enhanced expression of GFP suggested autophagosomes accumulation, indicating impaired autophagy. The CQ (positive control) also showed increased GFP-LC3B protein expression, Figure 3i. Apart, from AML-12 cells, we also performed a few experiments on HepG2 cells and found similar results. PA produced a defect in autophagy process, dose-dependently in HepG2 cells, as shown by p62 accumulation and reduced expression of Atg7, and Beclin-1, (Supplementary Figure 1a). Lysotracker-Green imaging of AML-12 cells, exposed to PA showed reduced staining, Figure 3g. These collective results indicate defective cellular autophagy by PA exposure in AML-12 cells and HepG2 cells. Treatment with TG prevented impairment of autophagy in PA exposed cells. MDC staining showed fewer autophagosomes accumulation in TG treated PA exposed AML-12 cells, followed by increased intensity of Lysotracker-Green dye, as compared to only PA exposed AML-12 cells, Figure 3g, h. TG treatment induced the phosphorylation of AMPK (#

represents p< 0.05 PA Vs. PA+TG 25 µM/50 µM), Figure 3c, 3e, along with Beclin-1 up-regulation ($^{\#}$ represents p< 0.05 PA Vs. PA+TG 25 µM/50 µM), and degradation of p62 ($^{\#\#\#}$represents p< 0.0001 PA Vs. PA+TG 25 µM/50 µM). All these observations with TG correlated well with the Everolimus (autophagy inducer). Further, in RFP-GFP-LC3B puncta assay, TG treated PA exposed cells showed enhanced RFP-LC3B protein expression (formation of autolysosomes) and reduced GFP-LC3B, suggesting normal autophagy process, Figure 3i. TG also complemented its autophagy restoring action in PA exposed HepG2 cells, which showed enhanced phosphorylation of AMPK, associated with up-regulation of Beclin-1, Atg7, and degradation of p62 (Supplementary Figure -1b).

3.6 TG failed to prevent LDs accumulation in the presence of autophagy inhibitors.

We tested the effect of TG in the presence of CQ and 3-MA in the AML-12 cells. In the presence of CQ and 3-MA, TG treatment could not prevent the LDs accumulation in PA exposed cells (n.s. represents p>0.05, PA Vs. PA+TG 50µM+CQ/PA+TG 50µM +3-MA). In cells treated with CQ and 3-MA only, LDs accumulation was significantly higher as compared to control cells (*** represents p< 0.0001 CQ Vs. Control and 3-MA Vs. Control), Figure 4a, 4b. The Trig content was also increased by 5-fold in PA exposed cells (*** represents p< 0.0001 PA Vs. Control), but in TG pre-treated cells it was significantly lowered ($^{\#\#\#}$ represents p< 0.0001 PA Vs. PA+TG 25 µM /50 µM). The Trig content was significantly higher in PA exposed cells treated with CQ and 3-MA, as compared to PA exposed cells only ($^{!!!}$ represents p<0.0001, PA Vs. PA + CQ, and PA Vs. PA + 3-MA). The AML-12 cells incubated with CQ and 3-MA, had a 4-fold rise in Trig content which was not significantly reduced by TG treatment, as compared to PA exposed cells only (n.s. represents p>0.05, PA Vs. PA+TG 25µM /50µM+CQ and PA Vs. PA+TG 25 µM /50µM +3-MA), Figure 4c. The protein expression of p62 (via ICC) in CQ treated cells, in the presence and absence of PA

and TG was determined. The p62 expression was increased, suggesting autophagosomes accumulation in cells only exposed to PA. CQ treated cells also showed accumulated autophagosomes, suggesting inhibition of autophagy. Along with p62, the cells were co-stained with the Nile Red dye, and the intensity of Nile Red dye significantly correlated with the expression of p62. In PA and CQ treated cells, there was an increased intensity of Nile Red fluorescence, along with p62 accumulation, which suggested inhibition of autophagy leading to LDs accumulation. TG treatment in PA exposed cells prevented autophagosomes accumulation shown by reduced expression of p62, and prevented the LDs accumulation, shown by low staining of Nile Red. The CQ prevented the lipid-lowering effect and autophagy restoring property of TG, as cells showed p62 accumulation and enhanced fluorescence intensity of Nile Red, similar to only PA exposed cells, Figure 4 D. This evidence clearly suggests that TG lipid-lowering effect in cells is associated with the induction of autophagy, and in the presence of autophagy inhibitors, the effectiveness of TG is diminished significantly.

3.7 Atg-7 silencing in HepG2 cells, accelerated lipogenesis, Trig accumulation and reduced the effect of TG.

The effect of TG was checked in Atg7-/- HepG2 cells, exposed to PA. We analysed the protein expression of Atg7, which was significantly negligible in HepG2 Atg7-/- cells as compared to control cells ($^{\alpha\alpha\alpha}$ represents $p<0.0001$, Atg7-/- cells Vs. Control), Figure 5a, 5c. Defective autophagy was further assured by the significant reduction in the expression of Beclin-1 in Atg7-/- cells, as compared to control cells,($^{\alpha\alpha\alpha}$ represents $p<0.0001$, Atg7-/- cells Vs. Control). Further, we analysed the expression of lipogenic proteins. In Atg7-/- cells, TG was unable to prevent the PA induced lipogenesis, shown by up-regulation of SREBP1 and PPAR-γ. The expression of PPAR-γ in PA exposed wild HepG2 cells was up by 2.5-fold

(*** represents p<0.0001, Atg7-/- cells Vs. Control cells), which was reduced in TG treated wild HepG2 cells. However, in Atg7-/- cells, the expression of PPAR-γ was not reduced significantly as compared to PA exposed wild HepG2 cells, (n.s. represents p>0.05, PA Vs. PA + TG 50µM + Atg7-/-), Figure 5a, 5c. Similar observations were seen with expression of SREBP1 (n.s. represents p>0.05, PA Vs. PA + TG 50µM + Atg7-/-, for SREBP1), Figure 5a, 5c. The Trig content in PA exposed Atg7-/- cells was significantly higher than PA exposed wild HepG2 cells ($^{!!}$ represents p<0.001, PA Vs. PA + Atg7-/-). Here, also TG treatment reduced the Trig content by 50% in HepG2 cells exposed to PA, as compared to un-treated PA exposed cells ($^{\#\#\#}$ represents p < 0.0001, PA Vs. PA + TG 50µM). However, in PA exposed Atg7-/- cells, treatment with TG did not reduce the Trig content as compared to control cells, ($^{\beta}$represents p<0.005, for PA+TG 50µM+ Atg7-/- Vs. Control) suggesting in-capability of TG action, due to non-induction of autophagy, Figure 5b. All these results, in which autophagy was inhibited either by employing CQ or 3-MA or by silencing of Atg7, showed that TG could not work effectively in preventing LDs accumulation. These results verify that TG mechanism of action is related to the alleviation of impaired autophagy in the cell, which is directly related to its anti-lipogenic effects.

3.8. TG prevented metabolic impairment, weight gain and insulin resistance in HC-HF-fed C57BL/6J mice.

The Group 2 mice, fed only on HC-HF diet showed significant weight gain, and increased serum cholesterol and Trig, as compared to Group 1 mice, who fed on SC diet only (*** represents p< 0.0001, Group 2 Vs. Group 1). Impaired lipid profile and weight gain were also associated with increased liver weights (** represents p< 0.0001, Group 2 Vs. Group 1), and development of insulin resistance, (*** represents p< 0.0001, Group 2 Vs. Group 1). TG treatment in Group 3 mice, which were fed on a HC-HF diet, had normal metabolic profile,

with significant reduction in weight gain, serum Trig and serum cholesterol levels ($^{###}$ represents $p< 0.0001$, Group 3 Vs. Group 2). In Group 3 mice, TG prevented HC-HF diet-induced insulin resistance, shown by low serum values of insulin, glucose, and HOMA-IR values ($^{###}$ represents $p < 0.0001$, Group 3 Vs. Group 2 for glucose, $^{#}$ represents $p<0.05$, Group 3 Vs. Group 2 for HOMA-IR, $^{##}$ represents $p<0.001$, Group 3 Vs. Group 2 for insulin), Table-I. These results indicate that TG treatment restored the metabolic impairments in Group 3 mice, which were profound in Group 2 mice.

3.9. HC-HF diet induced impaired lipophagy in livers of C57BL/6J mice, leading to hepatic steatosis.

The protein expression of autophagy and lipogenic markers, in liver tissue lysates of C57BL/6J mice, were studied. In, Group 2 mice the phosphorylation of AMPK and protein expression of AMPK was significantly reduced, as compared to Group 1 mice, (** represents $p<0.001$, Group 2 Vs. Group1), Figure 6a, 6b. The HC-HF diet fed mice of Group 2, showed p62 accumulation and down-regulation of Beclin-1, as compared to Group 1 mice, (*** represents $p< 0.0001$, Group 2 Vs. Group 1, for p62, * represents $p< 0.05$, Group 2 Vs. Group 1 for Beclin-1), Figure 6a, 6b. The hepatic protein expression of Srebp1, PPAR-γ, CD36, were significantly higher in Group 2 mice, as compared to Group 1,(*** represents $p< 0.0001$, Group 2 Vs. Group 1, for CD36, ** represents $p< 0.001$, Group 2 Vs. Group 1 for Srebp1, * represents $p< 0.05$, Group 2 Vs. Group 1 for PPAR- γ), Figure 6a, 6b.

Impaired hepatic autophagy in Group 2 mice was associated with the extensive lipid accumulation and formation of LDs. We studied the HLA by H&E staining and Nile Red staining of liver sections. H&E staining in Group 2 mice, showed severe macro and micro-vesicular steatosis (Black Arrows), a characteristic of NAFLD. However, Group 1 mice, showed normal liver parenchyma with minimal steatosis. Nile Red imaging of liver sections,

co-stained with DAPI dye, also showed higher fluorescence, in Group 2 mice, as compared to Group 1 mice, which indicates extensive LDs accumulation due to HC-HF feeding, Figure 6c, and 6d. Hence, these results suggest that HC-HF diet produced hepatic steatosis, due to increased denovo-lipogenesis via impairment of hepatic autophagy.

3.10 TG treatment prevented HLA, hepatic denovo-lipogenesis, in C57BL/6J mice, by activating AMPK induced hepatic autophagy.

TG treatment to HC-HF fed Group 3 mice, showed remarkable prevention from steatosis, with significantly reduced hepatic denovo-lipogenesis, and restored hepatic autophagy. Hepatic protein expression showed up-regulated Beclin-1, and degraded p62 which were significantly differed from Group 2 mice, ($^{###}$represents $p<0.0001$, for p62, Group 3 Vs. Group 2, $^{#}$represents $p<0.05$, for Beclin-1, Group 3 Vs. Group 2), Figure 6a, 6b, 6b. TG prevented the HC-HF associated reduced phosphorylation of AMPK, ($^{#}$represents $p<0.05$, Group 3 Vs. Group 2), Figure 6a, 6b.

Further, protein level of Srebp1 was reduced by 35% in Group 3 as compared to Group 2 ($^{##}$ represents $p<0.001$, Group 3 Vs. Group 2), and levels of PPAR-γ and CD36 were reduced by 45% and 60% respectively in Group 3 as compared to Group 2 ($^{##}$ represents p<0.001, Group 3 Vs. Group 2 for PPAR-γ, and $^{###}$ represents p<0.0001, Group 3 Vs. Group 2 for CD36), Figure 6a, 6b. TG treatment prevented the HLA in Group 3 mice as compared to Group 2. The H&E image of the liver section of Group 3 mice, showed reduced steatosis as compared to Group 2 mice, Figure 6c. It was further verified in Nile Red imaging in which Group 3 mice showed significantly fewer LDs as compared to Group 2, Figure 6d. Hence, these results confirmed that lipid accumulation due to HC-HF diet was associated with impairment of hepatic autophagy and enhanced lipid accumulation. TG treatment prevented the HLA in

HC-HF fed mice, by restoring hepatic autophagy and subsequently reducing the denovo-lipogenesis.

4. **Discussion**

TG is a traditional alkaloidal drug, which is a significant component of fenugreek seeds (Al-Habori et al., 2001). Many studies have confirmed its anti-diabetic and anti-oxidant properties (Genet et al., 2002; Hamadi, 2012; Zhou et al., 2012; Zhou et al., 2013). It was also shown to prevent adipocyte differentiation and lipid accumulation in pancreatic cells (Ilavenil et al., 2014). In this study, we evaluated the TG for its anti-steatotic ability, and further evaluated its mechanism. We have previously shown that PA stimulated hepatocytes bear autophagy blockade, which leads to lipid accumulation and lipo-toxicity (JLR). Here, it is evaluated in livers of C57BL/6J mice, fed with HC-HF diet. Further, the role of TG in modulating the cellular autophagy was studied. *De novo* lipogenesis and IR play a crucial role in the induction of HLA and precipitating steatosis (Diraison et al., 2003). Recent studies have shown that altered autophagy promotes LDs accumulation, leading to NAFLD and NASH (Dong and Czaja, 2013; Singh et al., 2009). In clinical settings liver samples of NASH patients, have also exhibited impaired autophagy (Amir and Czaja, 2011). In this study, we have demonstrated that impaired hepatic autophagy leads to enhanced *de novo* lipogenesis, which contributes to steatosis. Disruption of cellular autophagy by using Atg7 siRNA, and autophagy inhibitors (CQ and 3-MA) were correlated with the HLA, Trig content and denovo-lipogenesis in the cells. The ability of TG in preventing lipid accumulation and lipo-toxicity was examined, along with its role in modulating impaired autophagy.

Lipid accumulation and related lipo-toxicity, are the hallmark of fatty liver associated liver damage. So, initially, we evaluated TG for its anti-lipo-toxic, and anti-lipid accumulating potential in PA stimulated cells. TG prevented the PA-induced lipid accumulation and lipo-toxicity in AML-12 cells, as shown by Nile Red staining, altered $\Delta\Psi m$, and low bcl-2/bax

ratio. The anti-apoptotic activity of TG has been proved in other diabetes and cardiac-related pathologies (Ghule et al., 2012; Ilavenil et al., 2015). Further, the anti-lipoapoptotis activity of TG, was similar to the other pre-clinically proven anti-NAFLD agents (Love et al., 2017; Nissar et al., 2017). ER stress also mediates lipid accumulation in cells (Cnop et al., 2012). ER stress inducers viz. Thapsigargin and Tunicamycin have shown to induce lipid accumulation in the pancreatic, adipocytes and hepatic cells (Kammoun et al., 2009; Kim et al., 2005; Ozcan et al., 2006). In this study, PA induced ER stress in AML-12 cells, after 12 hours of exposure, similar to other studies, in which free fatty acids viz. PA, linolenic acid induced ER stress in liver cells, (Cui et al., 2013; Zhang et al., 2012) which led to lipid accumulation and lipo-toxicity. TG prevented the PA stimulated ER stress and ROS generation in AML-12 cells, which was confirmed by reduced levels of ER stress markers. This mechanism of TG has also been shown responsible for its anti-diabetic properties (Genet et al., 2002). Here, we show these effects as a preventive mechanism for steatosis. PA exposure to AML-12 cells, also resulted in dysfunctional anti-oxidant machinery as suggested by low levels of NRF-2 & SOD. However, TG pre-treated cells had normalized protein levels of NRF-2 and SOD. These effects of TG, correlated with the other agents, viz. 4-phenyl butyric acid (4-PBA), anti-oxidants and betaine supplements, which have proved their anti-steatotic potential (Dey and Lakshmanan, 2013; Kwon et al., 2009; Nissar et al., 2017). *De novo* lipogenesis is majorly involved in HLA and steatosis, which is regulated by mTOR (Caron et al., 2015). PA exposure to AML-12 cells, led to mTOR up-regulation, which induced enhanced lipo-genesis, revealed from up-regulated lipogenic markers. This process, led to the excess accumulation of LDs, demonstrated by increased expression of Perilipin and CD36, and also by Nile red staining. The mTOR up-regulation, and its role in lipogenesis has also been demonstrated and reviewed previously (Han and Wang, 2018; Laplante and Sabatini, 2009; Love et al., 2017). TG treatment prevented the mTOR up-regulation in PA

exposed AML-12 cells, leading to checking in lipogenesis, and reduced lipid accumulation. Similarly, many other drugs have shown to target lipogenesis and related proteins, in hepatocytes to prevent NAFLD (Ben-Shlomo et al., 2011; Dal Rhee et al., 2012; Kwon et al., 2009; Zhong et al., 2013).

The mTOR is a key regulator of autophagy and it's up-regulation, leads to autophagy inhibition (Alers et al., 2012). PA induced the up-regulation of mTOR, so we checked the autophagy pathway of the exposed cell, by analysing key autophagy proteins, and detected the autophagosomes and autolysosomes in cells. MDC staining showed autophagosomes accumulation in PA exposed cells. Accumulation of p62 and reduction in Atg 7 protein expression further confirmed the suppressed autophagy in cells due to lipid overload. The accumulation of p62 has been positively correlated with the Atg7 deficiency in the cells (Takamura et al., 2011). Beclin-1, which helps in the nucleation step of autophagy, was also down-regulated by PA exposure. These findings were similar to our previous study, which was done on Huh-7 cells (Nissar et al., 2017). However, in this study, we complemented the PA-induced autophagic blockade in HepG2 cells. The reduced autophagy correlated well with the PA induced decreased phosphorylation of AMPK. However m-TOR inhibitors act as autophagy inducers (Shintani and Klionsky, 2004) and activate AMPK, which facilitates autophagy via acting on the ULK-1 complex which accelerates the biogenesis of autophagosomes (Kim et al., 2011). The defect in autophagy was associated with LDs accumulation and increased Trig content in cells. We co-stained the LysoTracker green with Nile Red stain, to correlate the autophagy process with LDs mobilisation. We found that the high intensity of Nile red stain (LDs accumulation) complemented with low fluorescence of LysoTracker green stain (suggest impaired autophagic flux) in PA exposed AML-12 cells.

Moreover, RFP-GFP-LC3B punctate assay further, confirmed the autophagy blockade by PA, as there was an enhanced intensity of GFP-LC3B channel, in PA exposed cells, comparable with the positive control CQ. Further the use of autophagy inhibitors CQ and 3-MA increased the LDs and Trig content significantly in the cells. These results confirmed that there is an inverse correlation between impaired lipophagy, LDs accumulation and increased cellular Trig levels. The report suggests, that excess LDs accumulation in the cells lose the ability to degrade Trig, via lipophagy, which further leads to impaired lipid metabolism and promoting lipid accumulation (Ward et al., 2016). However, there is still unclear, that whether suppressed autophagy represents a cause of liver injury, or it's a result of liver damage. Another study showed that levels of Rubicon, an autophagy inhibiting protein was elevated in livers of NAFLD patients. Further the Rubicon knockout mice exhibited restored hepatic lipophagy with low Trig levels and lesser LDs accumulation (Schulze et al., 2015). So, in this study we tested that whether the anti-steatotic ability of TG is autophagy-mediated. TG treatment prevented the PA-induced impaired autophagic flux, which was confirmed in a number of experiments. The autophagosomes accumulation was reduced in TG treated AML-12 cells shown by MDC stain. LysoTracker green staining also showed enhanced intensity suggesting normal autophagy machinery.

Further, there was increased expression of Beclin-1 and reduced p62 expression in pre-TG treated and PA exposed cells. The expressions of Atg7 was also increased in TG treated cells, in comparison to only PA exposed cells. Moreover, the formation of autolysosomes was confirmed by RFP-GFP-LC3B punctate assay, which showed-enhanced RGP-LC3B intensity by TG treatment, which suggested normal functioning of autophagy, which was comparable with the Everolimus, a known autophagy inducer. TG also increased the phosphorylation of AMPK, which could also be the plausible reason for the restoration of autophagy. This effect was further complemented with the down-regulation of mTOR in TG pre-treated cells. In

short, the TG effect of autophagy normalization due to lipid overload in cells is associated with enhanced AMPK and reduced mTOR activity. This effect was also correlated with the reduced LDs and low Trig levels in TG pre-treated cells. However, in the presence of CQ and 3-MA, the TG could not prevent the PA-induced LDs and increased Trig content in the cells. The increased p62 accumulation due to PA, in the presence of CQ was not reduced by TG, which also complemented with increased Nile Red intensity. This phenomenon further demonstrated that the ability of TG in preventing steatosis is related to the induction of hepatic autophagy. Further, the silencing of Atg7 in HepG2 cells, led to enhanced lipid accumulation and increased Trig content in the cells. It was also accompanied by enhanced lipogenesis. In Atg7-/- cells, TG did not prevent PA-induced lipid accumulation and associated lipogenesis. The experiments in which we inhibited cellular autophagy, by using either CQ or 3-MA or by Atg7-/-, suggested us that impaired autophagy led to increased lipogenesis and lipid accumulation, which reduced the ability of TG in preventing the lipid accumulation.

Further, we tested the anti-steatotic potential of TG and its autophagy restoring potential in C57BL/6J mice, fed on SC and HC-HF diets for 16 weeks. HC-HF diet-induced metabolic impairments, increased weight gain in Group 2 mice, similar to the previous study (Love et al., 2017). However, in our previous study we did not study the hepatic autophagy concerning HC-HF diet administration to C57BL/6J mice. The HC-HF diet-induced impaired autophagy in livers of C57BL/6J mice, confirmed by increased hepatic p62 accumulation and reduced expression of Beclin-1, and reduced p-AMPK activity, which correlated with increased lipogenesis and increased hepatic Trig content. The impaired autophagy and enhanced lipogenesis in Group 2 livers, led to macro and micro vesicular steatosis. TG treatment to HC-HF fed Group 3 mice, prevented metabolic impairments, weight gain and resulted in an improved insulin-glucose profile in Group 3 mice. Liver tissue from mice within Group 3 had

minimal steatosis, and a significantly reduced Trig content, which may be attributed to enhanced p-AMPK/AMPK activity related hepatic autophagy normalization. The hepatic p62 accumulation was reduced in samples taken from mice in Group 3 along with Beclin-1 up-regulation. Nile Red staining also revealed fewer LDs accumulation in Group 3 livers, compared to Group 2. Hence, the findings in C57BL/6J mice, concerning autophagy impairment, lipid accumulation and TG effect were consistent with the result of *in-vitro* studies performed on AML-12 cells and HepG2 cells. Figure 7 summarises the study, by explaining the link between HC-HF diet induced impaired hepatic autophagy and role of TG in hepatic autophagy restoration.

5. Conclusion

This study explains the link between defective hepatic autophagy and enhanced denovo-lipogenesis. Excess nutrient supply via HC-HF diet led to impaired hepatic autophagy and steatosis. PA exposure also induced impaired autophagy and lipo-toxicity in AML-12 and HepG2 cells. TG treatment in PA stimulated cells, and HC-HF fed mice, prevented steatosis, by restoration of cellular autophagy and alleviation of ER and oxidative stress. Finally, this study shows the novel detailed mechanism of TG, in preventing NAFLD, which has the potential for use, as a therapeutic agent to treat it. This study also warrants the future clinical trial of TG to verify these experimental findings.

6. Conflict of Interest

Authors state no conflict of interest.

7. Funding

This study was funded by Council of Scientifica and Industrial Research (CSIR)-India, via grant number GAP-1122.

8. Acknowledgement

The stipend to LS and NAL from DST and UGC, respectively is acknowledged. Inputs and help from other members of the laboratory and the institute is highly acknowledged. Financial support by Council of Scientific and Industrial Research, CSIR-India, (GAP-1122) for the study is acknowledged. Support from Newton-Bhabha fund, by British council UK, and DBT India is also acknowledged.

9. Authors' Contributions

Love Sharma performed the main experiments, maintained the cell cultures, mice and wrote the manuscript.

Nazir A lone performed the silencing and knock down experiments and help in maintaining study mice groups.

Rachel M Knott helped in microscopy experiments and in the critical editing of the manuscript.

Adil Hassan helped in histopathology work and assessment.

Sheikh Tasduq Abdullah formulated the research problem, wrote and edited the manuscript and obtained the funding for the project and supervised the research program.

10. References

Al-Habori, M., Raman, A., Lawrence, M.J., Skett, P., 2001. In vitro effect of fenugreek extracts on intestinal sodium-dependent glucose uptake and hepatic glycogen phosphorylase A. Journal of Diabetes Research 2, 91-99.

Alers, S., Löffler, A.S., Wesselborg, S., Stork, B., 2012. Role of AMPK-mTOR-Ulk1/2 in the regulation of autophagy: cross talk, shortcuts, and feedbacks. Molecular and cellular biology 32, 2-11.

Amir, M., Czaja, M.J., 2011. Autophagy in nonalcoholic steatohepatitis. Expert review of gastroenterology & hepatology 5, 159-166.

Anthoni, U., Christophersen, C., Hougaard, L., Nielsen, P.H., 1991. Quaternary ammonium compounds in the biosphereâ€"an example of a versatile adaptive strategy. Comparative Biochemistry and Physiology Part B: Comparative Biochemistry 99, 1-18.

Bellentani, S., Scaglioni, F., Marino, M., Bedogni, G., 2010. Epidemiology of non-alcoholic fatty liver disease. Digestive diseases 28, 155-161.

Ben-Shlomo, S., Zvibel, I., Shnell, M., Shlomai, A., Chepurko, E., Halpern, Z., Barzilai, N., Oren, R., Fishman, S., 2011. Glucagon-like peptide-1 reduces hepatic lipogenesis via activation of AMP-activated protein kinase. Journal of hepatology 54, 1214-1223.

Berlanga, A., Guiu-Jurado, E., Porras, J.A., Auguet, T., 2014. Molecular pathways in non-alcoholic fatty liver disease. Clinical and experimental gastroenterology 7, 221.

Biederbick, A., Kern, H.F., Elsasser, H.P., 1995. Monodansylcadaverine (MDC) is a specific in vivo marker for autophagic vacuoles. European journal of cell biology 66, 3-14.

Caron, A., Richard, D., Laplante, M., 2015. The roles of mTOR complexes in lipid metabolism. Annual review of nutrition 35, 321-348.

Chazotte, B., 2011. Labeling lysosomes in live cells with LysoTracker. Cold Spring Harbor Protocols 2011, pdb. prot5571.

Cnop, M., Foufelle, F., Velloso, L.A., 2012. Endoplasmic reticulum stress, obesity and diabetes. Trends in molecular medicine 18, 59-68.

Cui, W., Ma, J., Wang, X., Yang, W., Zhang, J., Ji, Q., 2013. Free fatty acid induces endoplasmic reticulum stress and apoptosis of ß²-cells by Ca2+/calpain-2 pathways. PLoS One 8, e59921.

Dal Rhee, S., Kim, C.-H., Park, J.S., Jung, W.H., Park, S.B., Kim, H.Y., Bae, G.H., Kim, T.J., Kim, K.Y., 2012. Carbenoxolone prevents the development of fatty liver in C57BL/6-Lep ob/ob mice via the inhibition of sterol regulatory element binding protein-1c activity and apoptosis. European journal of pharmacology 691, 9-18.

Dey, A., Lakshmanan, J., 2013. The role of antioxidants and other agents in alleviating hyperglycemia mediated oxidative stress and injury in liver. Food & function 4, 1148-1184.

Diraison, F., Moulin, P.H., Beylot, M., 2003. Contribution of hepatic de novo lipogenesis and reesterification of plasma non esterified fatty acids to plasma triglyceride synthesis during non-alcoholic fatty liver disease. Diabetes & metabolism 29, 478-485.

Dong, H., Czaja, M.J., 2013. Regulation of lipid droplets by autophagy. Trends in Endocrinology & Metabolism 22, 234-240.

Farrukh, M.R., Nissar, U.A., Afnan, Q., Rafiq, R.A., Sharma, L., Amin, S., Kaiser, P., Sharma, P.R., Tasduq, S.A., 2014. Oxidative stress mediated Ca2+ release manifests endoplasmic reticulum stress leading to unfolded protein response in UV-B irradiated human skin cells. Journal of dermatological science 75, 24-35.

Folwarczna, J., Aleksandra Janas, Maria Pytlik, Urszula Cegieła, Leszek Śliwiński, Zora Krivošíková, Kornélia Štefiková, and Martin Gajdoš., 2016. Effects of trigonelline, an alkaloid present in coffee, on diabetes-induced disorders in the rat skeletal system. Nutrients 8, 133.

Gaggini, M., Morelli, M., Buzzigoli, E., DeFronzo, R.A., Bugianesi, E., Gastaldelli, A., 2013. Non-alcoholic fatty liver disease (NAFLD) and its connection with insulin resistance, dyslipidemia, atherosclerosis and coronary heart disease. Nutrients 5, 1544-1560.

Genet, S., Kale, R.K., Baquer, N.Z., 2002. Alterations in antioxidant enzymes and oxidative damage in experimental diabetic rat tissues: effect of vanadate and fenugreek (Trigonella foenum graecum). Molecular and cellular biochemistry 236, 7-12.

Ghule, A.E., Jadhav, S.S., Bodhankar, S.L., 2012. Trigonelline ameliorates diabetic hypertensive nephropathy by suppression of oxidative stress in kidney and reduction in renal cell apoptosis and fibrosis in streptozotocin induced neonatal diabetic (nSTZ) rats. International immunopharmacology 14, 740-748.

Greenberg, A.S., Coleman, R.A., Kraemer, F.B., McManaman, J.L., Obin, M.S., Puri, V., Yan, Q.-W., Miyoshi, H., Mashek, D.G., 2011. The role of lipid droplets in metabolic disease in rodents and humans. The Journal of clinical investigation 121, 2102-2110.

Hamadi, S.A., 2012. Effect of trigonelline and ethanol extract of Iraqi Fenugreek seeds on oxidative stress in alloxan diabetic rabbits. Journal of the Association of Arab Universities for Basic and Applied Sciences 12, 23-26.

Han, J., Wang, Y., 2018. mTORC1 signaling in hepatic lipid metabolism. Protein & cell, 1-7.

Heid, H., Rickelt, S., Zimbelmann, R., Winter, S., Schumacher, H., DÃ-rflinger, Y., Kuhn, C., Franke, W.W., 2014. On the formation of lipid droplets in human adipocytes: the organization of the perilipin-vimentin cortex. PLoS One 9, e90386.

Huang, S.-P., Chien, J.-Y., Tsai, R.-K., 2015. Ethambutol induces impaired autophagic flux and apoptosis in the retina. Disease models & mechanisms, dmm. 019737.

Ilavenil, S., Arasu, M.V., Lee, J.-C., Kim, D.H., Roh, S.G., Park, H.S., Choi, G.J., Mayakrishnan, V., Choi, K.C., 2014. Trigonelline attenuates the adipocyte differentiation and lipid accumulation in 3T3-L1 cells. Phytomedicine 21, 758-765.

Ilavenil, S., Kim, D.H., Jeong, Y.-I., Arasu, M.V., Vijayakumar, M., Prabhu, P.N., Srigopalram, S., Choi, K.C., 2015. Trigonelline protects the cardiocyte from hydrogen peroxide induced apoptosis in H9c2 cells. Asian Pacific journal of tropical medicine 8, 263-268.

Kammoun, H.l.n.L., Chabanon, H., Hainault, I., Luquet, S., Magnan, C., Koike, T., FerrÃ©, P., Foufelle, F., 2009. GRP78 expression inhibits insulin and ER stressâ€“induced SREBP-1c activation and reduces hepatic steatosis in mice. The Journal of clinical investigation 119, 1201-1215.

Kim, A.J., Shi, Y., Austin, R.C., Werstuck, G.H., 2005. Valproate protects cells from ER stress-induced lipid accumulation and apoptosis by inhibiting glycogen synthase kinase-3. J Cell Sci 118, 89-99.

Kim, J., Kundu, M., Viollet, B., Guan, K.-L., 2011. AMPK and mTOR regulate autophagy through direct phosphorylation of Ulk1. Nature cell biology 13, 132.

Kwon, D.Y., Jung, Y.S., Kim, S.J., Park, H.K., Park, J.H., Kim, Y.C., 2009. Impaired sulfur-amino acid metabolism and oxidative stress in nonalcoholic fatty liver are alleviated by betaine supplementation in rats. The Journal of nutrition 139, 63-68.

Laplante, M., Sabatini, D.M., 2009. An emerging role of mTOR in lipid biosynthesis. Current Biology 19, R1046-R1052.

Love, S., Mudasir, M.A., Bhardwaj, S.C., Singh, G., Tasduq, S.A., 2017. Long-term administration of tacrolimus and everolimus prevents high cholesterol-high fructose-induced steatosis in C57BL/6J mice by inhibiting de-novo lipogenesis. Oncotarget 8, 113403.

Miquilena-Colina, M.E., Lima-Cabello, E., SÃ¡nchez-Campos, S., GarcÃa-Mediavilla, M.V., FernÃ¡ndez-Bermejo, M., Lozano-RodrÃguez, T., Vargas-CastrillÃ³n, J., BuquÃ©, X., Ochoa, B.a., Aspichueta, P., 2011. Hepatic fatty acid translocase CD36 upregulation is

associated with insulin resistance, hyperinsulinaemia and increased steatosis in non-alcoholic steatohepatitis and chronic hepatitis C. Gut, gut. 2010.222844.

Nissar, A.U., Sharma, L., Mudasir, M.A., Nazir, L.A., Umar, S.A., Sharma, P.R., Vishwakarma, R.A., Tasduq, S.A., 2017. Chemical chaperone 4-phenyl butyric acid (4-PBA) reduces hepatocellular lipid accumulation and lipotoxicity through induction of autophagy. Journal of lipid research 58, 1855-1868.

Nissar, A.U., Sharma, L., Tasduq, S.A., 2015. Palmitic acid induced lipotoxicity is associated with altered lipid metabolism, enhanced CYP450 2E1 and intracellular calcium mediated ER stress in human hepatoma cells. Toxicology Research 4, 1344-1358.

Ouyang, L., Shi, Z., Zhao, S., Wang, F.-T., Zhou, T.-T., Liu, B., Bao, J.-K., 2012. Programmed cell death pathways in cancer: a review of apoptosis, autophagy and programmed necrosis. Cell proliferation 45, 487-498.

Ozcan, U., Yilmaz, E., Ozcan, L., Furuhashi, M., Vaillancourt, E., Smith, R.O., 2006. Chemical chaperones reduce ER stress and restore glucose homeostasis in a mouse model of type 2 diabetes. Science 313, 1137-1140.

Perez-Neut, M., Haar, L., Rao, V., Santha, S., Lansu, K., Rana, B., Jones, W.K., Gentile, S., 2016. Activation of hERG3 channel stimulates autophagy and promotes cellular senescence in melanoma. Oncotarget 7, 21991.

Quan, H.Y., Kim, S.J., Jo, H.K., Kim, G.W., Chung, S.H., 2013. Betulinic acid alleviates non-alcoholic fatty liver by inhibiting SREBP1 activity via the AMPKâ€“mTORâ€“SREBP signaling pathway. Biochemical pharmacology 85, 1330-1340.

Rah, B., Rasool, R.u., Nayak, D., Yousuf, S.K., Mukherjee, D., Kumar, L.D., Goswami, A., 2015. PAWR-mediated suppression of BCL2 promotes switching of 3-azido withaferin A (3-AWA)-induced autophagy to apoptosis in prostate cancer cells. Autophagy 11, 314-331.

RodrÃ-guez-Sureda, V.c., Peinado-Onsurbe, J., 2005. A procedure for measuring triacylglyceride and cholesterol content using a small amount of tissue. Analytical biochemistry 343, 277-282.

Schulze, R.J., Sathyanarayan, A., Mashek, D.G., 2015. Breaking fat: the regulation and mechanisms of lipophagy. Biochimica et Biophysica Acta (BBA)-Molecular and Cell Biology of Lipids 1862, 1178-1187.

Shintani, T., Klionsky, D.J., 2004. Autophagy in health and disease: a double-edged sword. Science 306, 990-995.

Singh, R., Kaushik, S., Wang, Y., Xiang, Y., Novak, I., Komatsu, M., Tanaka, K., Cuervo, A.M., Czaja, M.J., 2009. Autophagy regulates lipid metabolism. Nature 458, 1131.

Sinha, R.A., Farah, B.L., Singh, B.K., Siddique, M.M., Li, Y., Wu, Y., Ilkayeva, O.R., Gooding, J., Ching, J., Zhou, J., 2014. Caffeine stimulates hepatic lipid metabolism by the autophagy-lysosomal pathway in mice. Hepatology 59, 1366-1380.

Takamura, A., Komatsu, M., Hara, T., Sakamoto, A., Kishi, C., Waguri, S., Eishi, Y., Hino, O., Tanaka, K., Mizushima, N., 2011. Autophagy-deficient mice develop multiple liver tumors. Genes & development 25, 795-800.

Tharaheswari, M., Reddy, N.J., Kumar, R., Varshney, K.C., Kannan, M., Rani, S.S., 2014. Trigonelline and diosgenin attenuate ER stress, oxidative stress-mediated damage in pancreas and enhance adipose tissue PPAR-γ activity in type 2 diabetic rats. Molecular and cellular biochemistry 396, 161-174.

Trovato, F.M., Martines, G.F., Brischetto, D., Catalano, D., Musumeci, G., Trovato, G.M., 2016. Fatty liver disease and lifestyle in youngsters: diet, food intake frequency, exercise, sleep shortage and fashion. Liver International 36, 427-433.

Um, S.H., D'Alessio, D., Thomas, G., 2006. Nutrient overload, insulin resistance, and ribosomal protein S6 kinase 1, S6K1. Cell metabolism 3, 393-402.

Ward, C., Martinez-Lopez, N., Otten, E.G., Carroll, B., Maetzel, D., Singh, R., Sarkar, S., Korolchuk, V.I., 2016. Autophagy, lipophagy and lysosomal lipid storage disorders. Biochimica et Biophysica Acta (BBA)-Molecular and Cell Biology of Lipids 1861, 269-284.

Wree, A., Broderick, L., Canbay, A., Hoffman, H.M., Feldstein, A.E., 2013. From NAFLD to NASH to cirrhosis-new insights into disease mechanisms. Nature Reviews Gastroenterology and Hepatology 10, 627.

Zeiger, E., Tice, R., 1997. Trigonelline; Review of Toxicological Literature. Research Triangle Park, North Carolina: National Institute of Environmental Health Sciences and Integrated Laboratory Systems, 27.

Zhang, Y., Chen, M.-l., Zhou, Y., Yi, L., Gao, Y.x., Ran, L., Chen, S.h., Zhang, T., Zhou, X., Zou, D., 2015. Resveratrol improves hepatic steatosis by inducing autophagy through the cAMP signaling pathway. Molecular nutrition & food research 59, 1443-1457.

Zhang, Y., Xue, R., Zhang, Z., Yang, X., Shi, H., 2012. Palmitic and linoleic acids induce ER stress and apoptosis in hepatoma cells. Lipids in health and disease 11, 1.

Zhong, D., Zhang, Y., Zeng, Y.-j., Gao, M., Wu, G.-z., Hu, C.-j., Huang, G., He, F.-t., 2013. MicroRNA-613 represses lipogenesis in HepG2 cells by downregulating LXRα. Lipids in health and disease 12, 32.

Zhou, J., Chan, L., Zhou, S., 2012. Trigonelline: a plant alkaloid with therapeutic potential for diabetes and central nervous system disease. Current medicinal chemistry 19, 3523-3531.

Zhou, J., Zhou, S., Zeng, S., 2013. Experimental diabetes treated with trigonelline: effect on β cell and pancreatic oxidative parameters. Fundamental & clinical pharmacology 27, 279-287.

Table -I: Effect of TG on metabolic and serum profile of mice fed with HC-HF diet.

Parameters	SC (Group1)	HC-HF (Group2)	HC-HF+TG (Group3)	SC+TG (Group4)
Weight (g)	29±2.3	45±2.4***	33±2.1$^{\#\#\#}$	29±1.9
Liver Weight (g)	1.32±0.4	2.69±0.3**	1.46±0.3$^{\#\#}$	1.2±0.2
Liver (% of body weight)	4.55±0.3	5.97±0.4***	4.56±0.4$^{\#\#\#}$	4.13±0.1
Serum Trig (mg/dl)	82.75±7.4	146.75±16***	91.5±6.75$^{\#\#\#}$	80.25±4.6
Serum Cholesterol (mg/dl)	103.25±10.2	267.25±11.2***	157±11.5$^{\#\#\#}$	104±4.7
Glucose (mg/dl)	165.75±26.3	354.75±47.3***	169±15.8$^{\#\#\#}$	161.75±6.0
Insulin (mIU/L)	1.98±0.4	4.3±0.8**	2.3±0.5$^{\#}$	2.1±0.3
HOMA-IR	0.81±0.2	3.76±0.2***	0.96±0.1$^{\#\#}$	0.83±0.1
Hepatic TG (mg/mg)	39.23±6.4	150.2±19.9***	83.2±12.52$^{\#\#\#}$	30.86±5.11

*Indicates comparison between SC (Group1) Vs. HC-HF (Group2). $^{\#}$ indicates comparison between HC-HF (Group2) Vs. HC-HF+TG (Group3).

Legend to Table-I

TG, prevented HC-HF diet induced metabolic impairments in C57BL/6J mice.HC-HF diet (Group2) induced significant weight gain, followed by HOMA-IR and elevated serum Cholesterol and Trig levels, as compared to SC diet (Group1). TG in Group3 mice, prevented the HC-HF diet induced metabolic impairments, HOMA-IR, and weight gain, due to HC-HF feeding. Results are shown as mean ± SEM. $p<0.05$, is considered significant. * denotes, SC (Group1) Vs. HC-HF (Group2), while $^{\#}$denotes, HC-HF(Group2) Vs. HC-HF+TG(Group3).

Figure Legends

Figure- 1

Effect of TG on PA-induced cytotoxicity and lipid accumulation: (A) Bar graph representing effect of TG on AML-12 cells, proliferation, after 24 hours of incubation and analysed via MTT assay. **(B)** Bar graph representing cell viability after 24 hours exposure of AML-12 cells, with PA-treated with and without the TG. **(C)** Images are showing JC-9 staining of AML-12 cells, exposed to PA for 24 hours, with and without 4 hours prior treatment with TG. **(D)** Images showing LDs accumulation performed via Nile Red staining, on AML-12 cells, exposed to PA for 24 hours, with and without 4 hours prior treatment of TG. **(D-1)** The bar graph is representing fold changes in intensity of Nile Red of Figure 1-D, analysed by Image J software . Results are expressed as mean ± SEM. *p*-value was determined by student *'t'* test, and considered significant for ≤ 0.05.

Figure-2

PA-induced ER stress, oxidative stress, and apoptosis in AML-12 cells, and effect of TG on PA-induced ER stress, oxidative stress and on apoptotic markers in PA exposed AML-12 cells: (A) Representative images (n=3) of western blots of grp-78, CHOP, elf2-a, total elf2-a , ATF-4 of AML-12 cells, after 12 hours exposure to PA and with and without treatment with TG.**(B)** Images, of H_2DCF-DA staining of AML-12 cells, after 12 hours exposure to PA and with and without treatment with TG, for detecting ROS generation. **(C)** Representative images (n=3) of western blots of cl-PARP, bcl-2, bax, and beta-actin, of AML-12 cells**,** after 24 hours exposure to PA and with and without treatment with TG. **(D).** The bar graph is representing fold changes in protein expressions of grp-78, elf2-a, bcl-2/bax and cl-PARP. Fold changes were calculated after densitometric analysis of three independent images of representative blots in Figure 2A and Figure 2C. The calculation was normalized to

their native actin, and fold change were calculated w.r.t. to expression of control untreated cells. Results are expressed as mean ±SEM. p-value was determined by student 't' test, and considered significant for ≤ 0.05.

Figure-3

PA-induced denovo-lipogenesis, LDs accumulation and impaired autophagy in AML-12 cells. TG treatment prevented PA induced impaired autophagy and reduced LDs accumulation : **(A) & (B)** Representative images (n=3) of western blots of p-mTOR, mTOR, p-Akt, Akt, Srebp1, PPAR-y, perilipin, CD36 and beta-actin, of AML-12 cells**,** after 24 hours exposure to PA and with and without treatment with TG. **(C)** Representative images (n=3) of western blots of beclin-1, p62, p-AMPK, AMPK, Atg7 and beta-actin, of AML-12 cells, after 24 hours exposure to PA and with and without treatment with TG. **(D)** The bar graphs are representing fold changes in protein expressions of p-mTOR/mTOR, p-Akt/Akt, Srebp1, PPAR-y, perilipin, and CD36. **(E)** Bar graphs are representing fold changes in protein expressions of beclin-1, p62, and p-AMPK/AMPK. Fold changes were calculated after densitometric analysis of three independent images of representative blots in Figure 3A, 3B, 3 E. The calculation was normalized to their native actin, and fold changes were calculated w.r.t. to expression of control untreated cells. **(F)** ICC images of Beclin-1 protein expression, co-stained with DAPI, on AML-12 cells, after 24 hours exposure to PA and with and without treatment with TG. The images were taken at 40X, on EVOS microscope using 100µM scale. **(G)** Representative photomicrographs of LysoTracker and Nile red co-stained AML-12, after indicated treatments, taken at 40X, on 50µM scale. **(H)** MDC staining images, for detecting autophagosomes, in AML-12 cells, after 24 hours exposure to PA and with and without treatment with TG. **(I)** Immunostaining of autophagosomes via RFP-GFP-LC3B puncta vector assay. The LC3 Vector, denotes that cells have been transfected with RFP-GFP-LC3B

Bacman 2.0 reagent, as per described protocol, in method section. Cells were transfected as per manufacturer's instructions and exposed to PA, CQ and/or TG as indicated. Imaging was done by EVOS, flourescene microscope at 40X lens, with 100µM scale. The images were taken at 20X, on EVOS microscope using 100µM scale. Results are expressed as mean ±SEM. p-value was determined by student 't' test, and considered significant for ≤ 0.05.

Figure-4

Effect of TG in presence and absence of autophagy inhibitors CQ and 3-MA, and RFP-GFP co-staining with LC3B vector, for puncta imaging: (A) Nile Red images of AML-12 cells, exposed to several treatments with either PA, CQ, 3-MA, and TG as indicated.The images were taken at 20X, on EVOS microscope using 100µM scale. **(B)** Bar graphs are representing fold change in Nile red intensity, considering Control image as 1. The images were analysed by Image J software, NIH. **(C)** Bar graphs representing Trig content, of AML-12 cells, exposed to several treatments as indicated. The Trig content was normalized by protein content of the cells, and calculations were converted in to fold changes, taking 1 for control un-treated cells. **(D)** ICC images showing p62 expression (Green) on AML-12 cells, co-stained with Nile Red and DAPI dye, after treatments with PA, CQ, and TG as indicated. The images were taken at 20X, using 100uM scale on Evos microscope. Results are expressed as mean ± SEM. *p*-value was determined by student 't' test, and considered significant for ≤ 0.05.

Figure -5

Atg7 silencing in HepG2 cells, with Atg7 siRNA. Effect of TG on Atg7 -/- cells, in the presence of PA. (A) Representative images (n=3) of western blots of beclin-1, p62, Srebp1, PPAR-y, Atg7 and beta-actin, of HepG2 cells, treated with PA, Atg7 siRNA, and TG in combination and alone as indicated. **(B)** Bar graph representing Trig content, of HepG2 cells,

exposed to several treatments as indicated. The Trig content was normalized by protein content of the cells, and calculations were converted in to fold changes, taking 1 for control un-treated cells. **(C)** Bar graph showing fold changes in protein expressions of PPAR-γ, beclin-1, Srebp1, and Atg7, calculated after normalizing with their respective Beta-actins. The calculation was done by densitometric analysis of the representative blots, shown in Figure 5-A, via Image Lab Software Bio-Rad. The protein expression for control untreated cells was taken as 1, for calculations of other treatments. Results are expressed as mean ± SEM. p-value was determined by student 't' test, and considered significant for ≤ 0.05.

Figure -6

TG prevented HC-HF diet-induced hepatic steatosis, hepatic autophagic blockade, and denovo-lipogenesis. (A) Representative western blots images (n=3) of liver protein lysates of C57BL/6J mice, for various proteins, as indicated. The 4 mice of each group were randomly selected, and liver lysates were prepared. The six liver lysates of different mice of each group were pooled to 2 lysate each and run in duplicates as shown in the figure. First two lanes for Group 1, next 3&4 lanes for Group 2, 5&6 for Group 3 and 7&8 for Group 4. **(B)** Bar graphs obtained after densitometric analysis of western blots for representative images shown in Figure 7A, by Image Lab software, Bio-Rad. The values were normalized to their corresponding beta-actins and converted in to fold changes, w.r.t. to Group 1, considering as 1. **(C)** Representative photo-micrographs of H&E staining (20X) of liver sections of C57BL/6J mice, with indicated treatments. **(D)** Representative photo-micrographs of Nile red imaging (20X) of liver sections, of C57BL/6J mice, also co-stained with DAPI dye. The scale at 100µM.

Figure-7

PA and/or HC-HF mediated autophagy blockade resulting in fatty liver. Effect of TG in preventing PA and/or HC-HF induced fatty liver, by restoring autophagy.

Green Arrows: Indicate up-regulation/induction, **Red Arrows**: Indicate down-regulation/inhibition/prevention.

Hepatic mTOR is stimulated due to PA exposure and HC-F diet. PA and HC-HF diet, itself impair autophagy and further, activate mTOR shuts the autophagy. Impaired hepatic autophagy is also inhibited due to reduced activity of AMPK, because of lipid overload. Impaired hepatic autophagy leads to LDs, accumulation and finally NAFLD. TG treatment prevented PA/HC-HF diet-induced mTOR up-regulation, restored AMPK levels, prevented the impairment of hepatic autophagy, and subsequently prevented the development of NAFLD.

Supplementary Figure-1

PA induced impaired autophagy and LDs accumulation in HepG2 cell and effect of TG on PA induced impaired autophagy. Effect of TG on anti-oxidant proteins, on PA exposed AML-12 cells. (A) Representative images (n=3) showing dose dependent effect of PA on LC-3II, p62 and Atg7 expression of HepG2 cells, via western blotting. **(B)** Representative images (n=3) of western blots of indicated proteins, showing effect of TG and Everolimus on PA exposed HepG2 cells. **(C)** Representative western blots (n=3), for effect of TG on PA induced alterations in protein expressions of Nrf-2, SOD, and Catalase, after 24 hours, of exposure to PA and/or pre-treatment with TG.

Figure-4

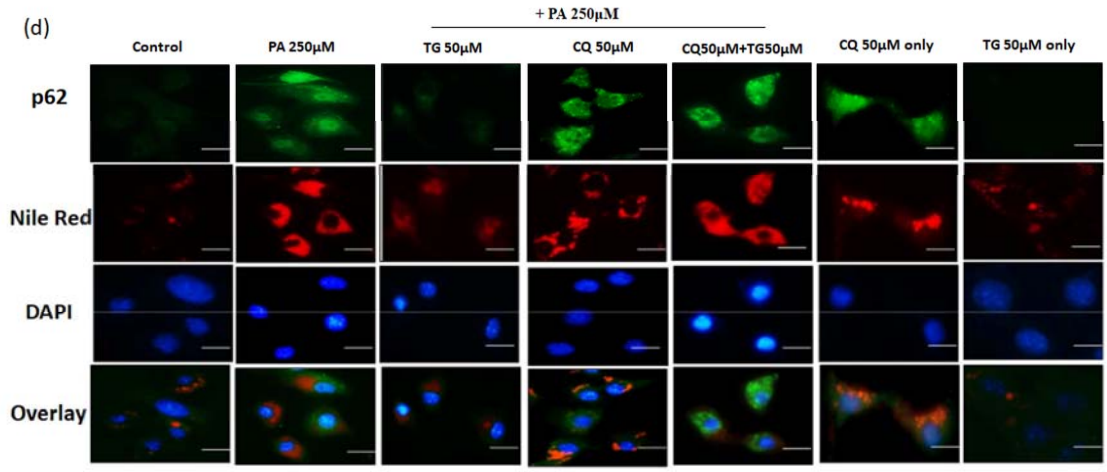

Figure -5

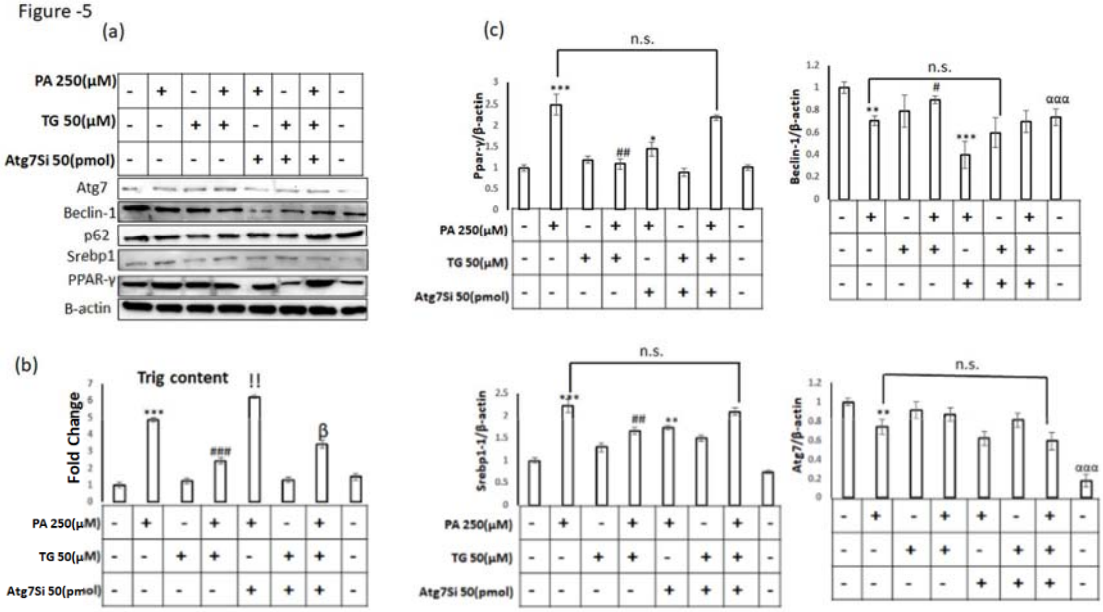

Figure 2

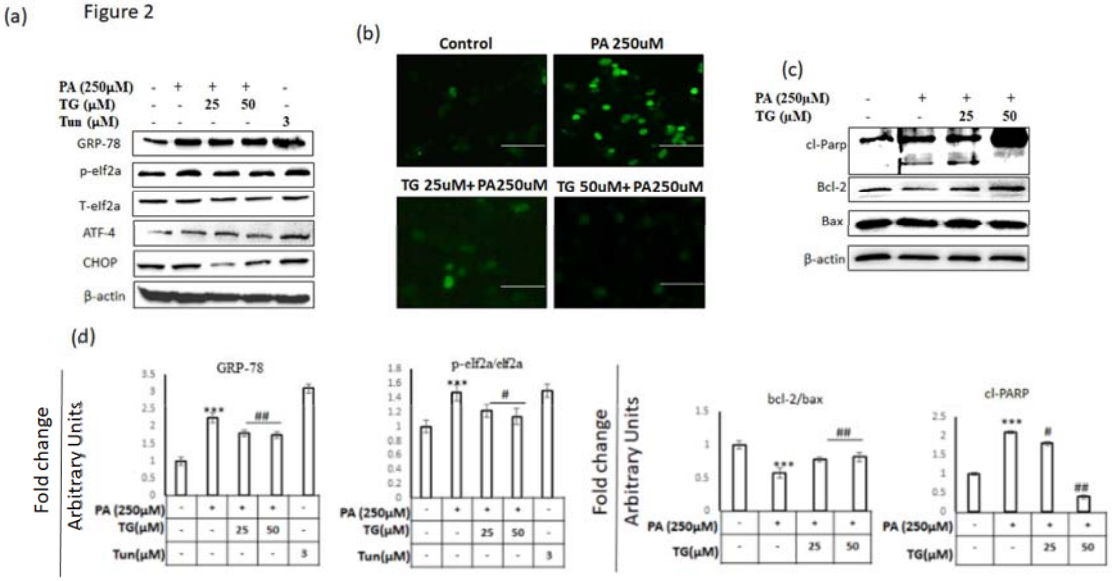

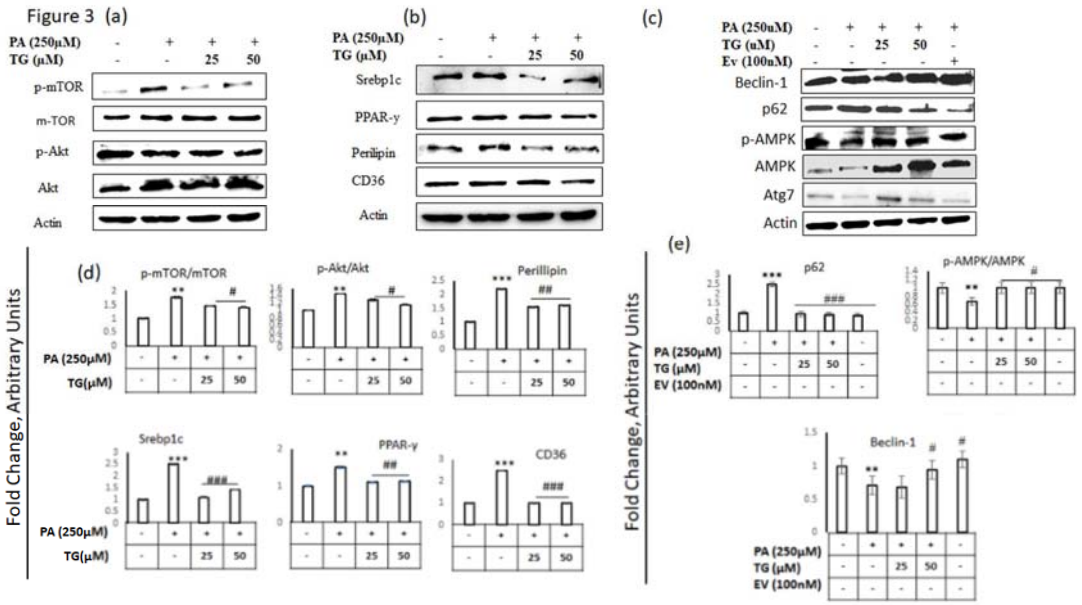

Figure-3

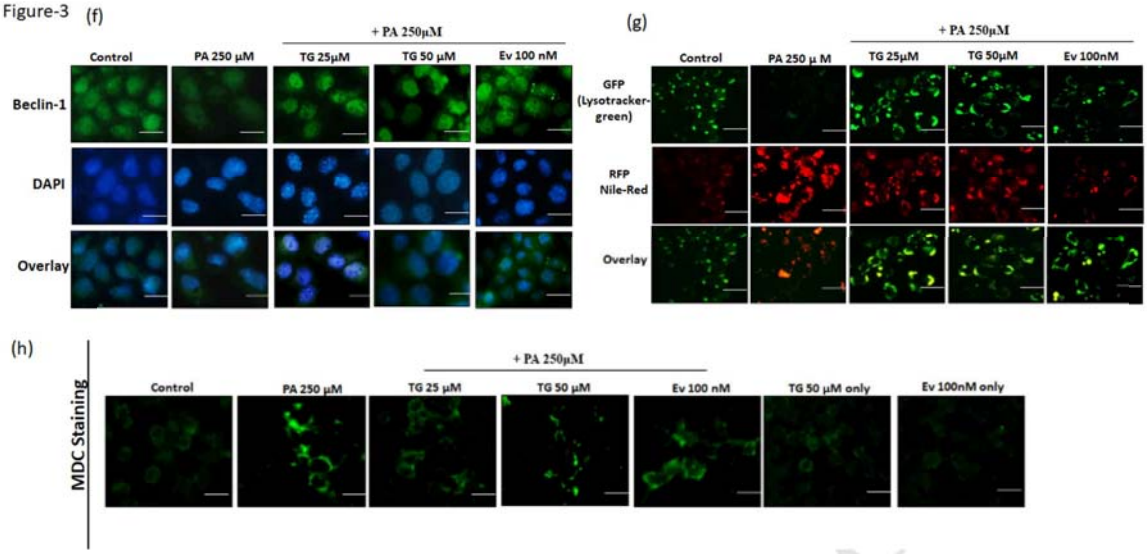

Figure-3 (i)

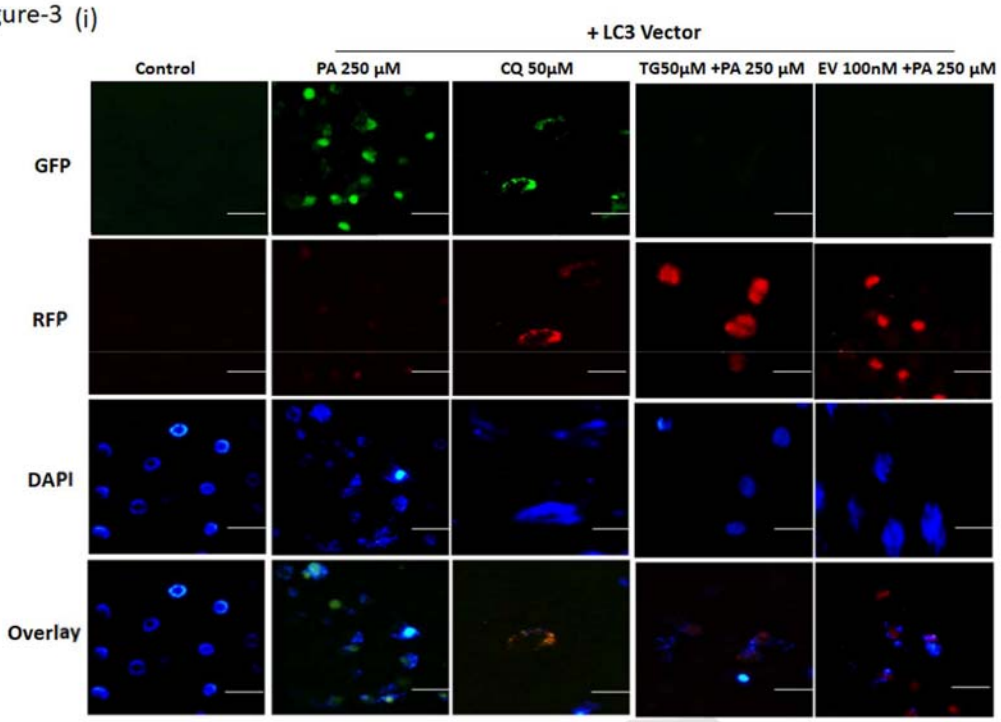

Figure-4

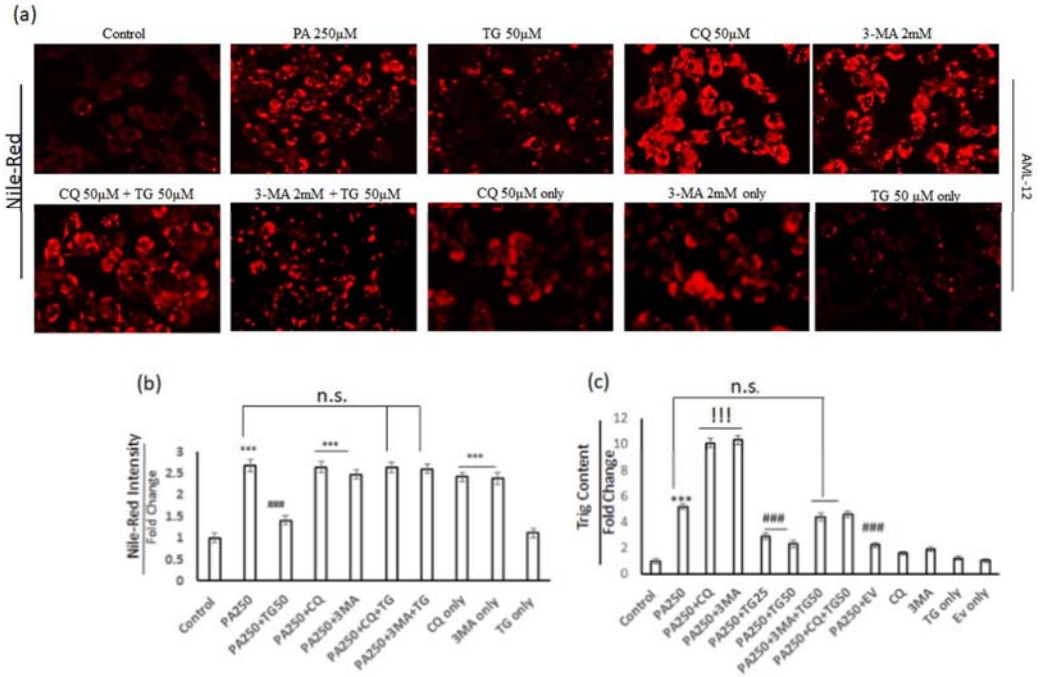

Figure 6

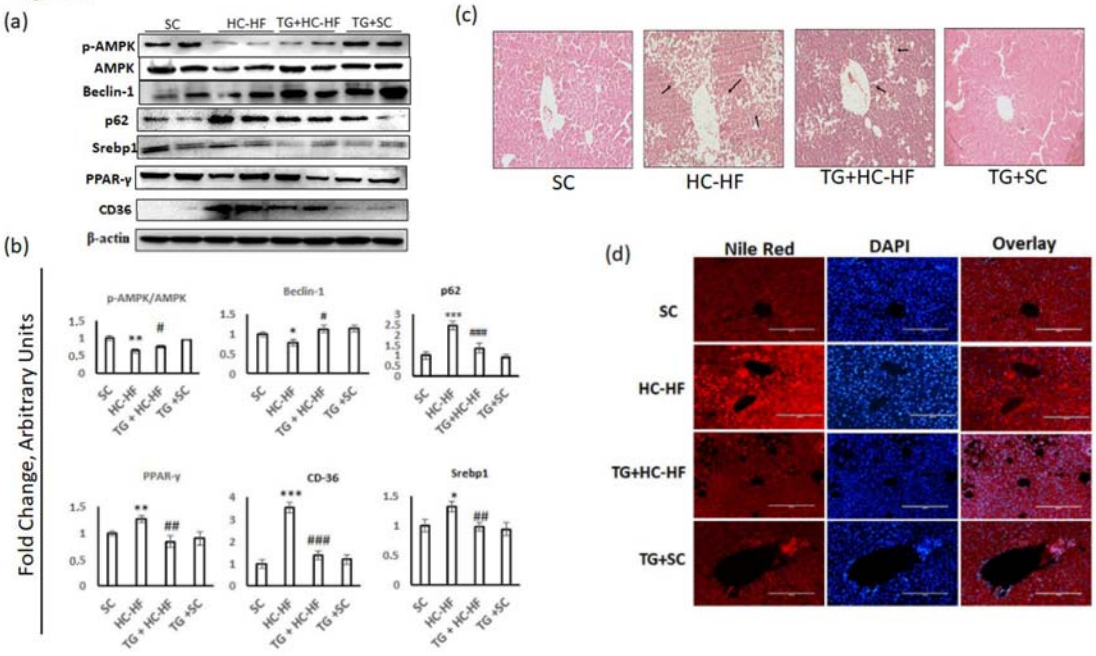

Figure 7

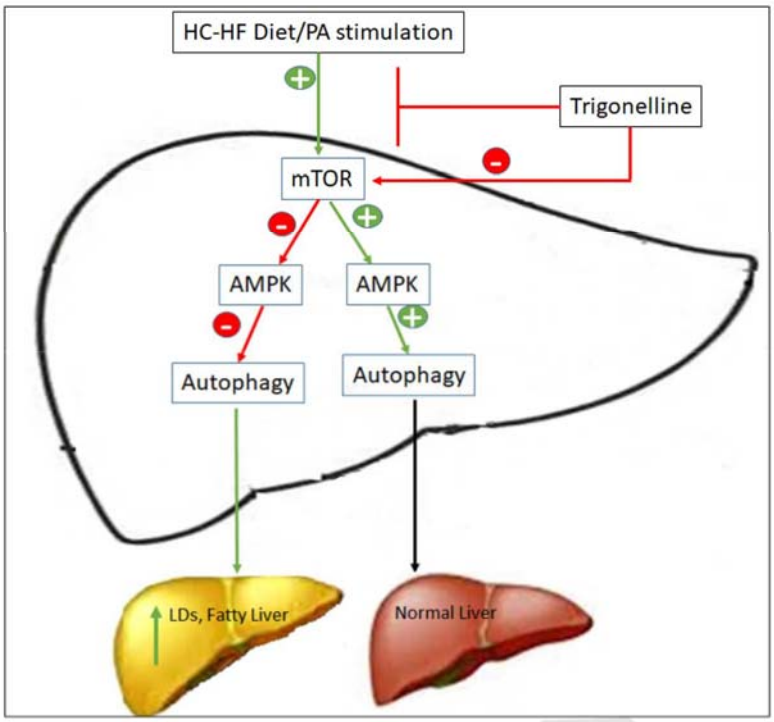

Figure 1

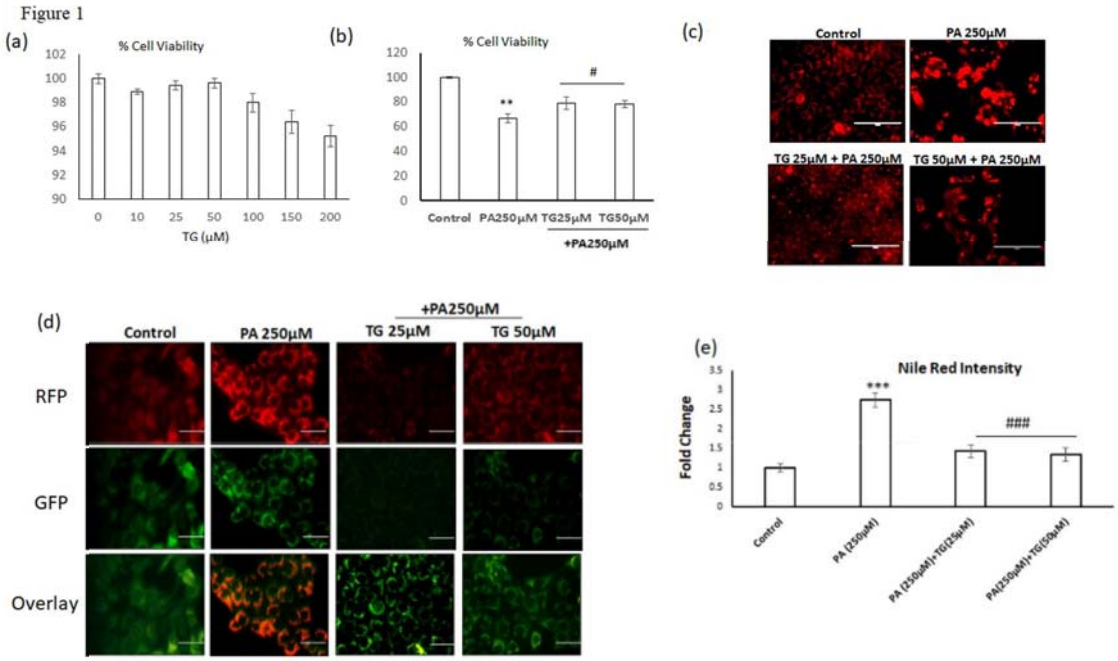

Highlights

- C57BL/6J mice fed with High Cholesterol-High Fat (HC-HF) diet exhibited suppressed hepatic autophagy, leading to steatosis.
- Palmitic acid (PA), also induced impaired autophagy in AML-12 and HepG2 cells, which led to lipid accumulation and lipo-toxicity.
- Trigonelline (TG) treatment restored the hepatic autophagy in HC-HF diet fed mice, and PA exposed cells, resulting in prevention of steatosis.
- Use of autophagy inhibitors, restricted the TG ability to restore autophagy in PA exposed cells.